PHYSICAL REVIEW D **72,** 115012 (2005)

Supersymmetric heavy Higgs bosons at e^+e^- linear collider and dark-matter physics

Takeo Moroi and Yasuhiro Shimizu

Department of Physics, Tohoku University, Sendai 980-8578, Japan

(Received 4 October 2005; published 19 December 2005)

We consider the capability of the e^+e^- linear collider (which has recently been called the International Linear Collider, or ILC) for studying the properties of the heavy Higgs bosons in the supersymmetric standard model. We pay special attention to the large $\tan\beta$ region which is motivated, in particular, by explaining the dark-matter density of the universe (i.e., so-called ''rapid-annihilation funnels''). We perform a systematic analysis to estimate expected uncertainties in the masses and widths of the heavy Higgs bosons assuming an energy and integrated luminosity of $\sqrt{s} = 1$ TeV and $L = 1$ ab^{-1}. We also discuss its implication to the reconstruction of the dark-matter density of the universe.

DOI: 10.1103/PhysRevD.72.115012 PACS numbers: 12.60.Jv, 13.66.Fg, 95.35.+d

I. INTRODUCTION

An e^+e^- linear collider, the International Linear Collier (ILC), has been discussed as a new experimental tool to study the physics at the electroweak scale and beyond [1–4]. The primary purpose of the ILC is to clarify the physics of the electroweak symmetry breaking and physics beyond the standard model; in order to solve the naturalness problem in the standard model, it is expected that some new physics will show up at the energy scale of 100 GeV–1 TeV. Discovery and, in particular, precise studies of such new physics should become very important once the ILC will be built. Thus, at the current stage, we should study the potential of the ILC for such purposes.

Among various possibilities, supersymmetry (SUSY) is one of the prominent candidates of the new physics beyond the standard model. Accordingly, superpartners of the standard-model particles are regarded as significant targets of the ILC. As well as the superparticles, however, we should also study another class of new particles which show up in the supersymmetric models, that is, the heavy Higgs bosons. Since the minimal supersymmetric standard model (MSSM) contains two Higgs doublets, i.e., up- and down-type Higgs bosons, CP even and odd neutral Higgs bosons (H and A) as well as the charged Higgses $H^\pm$ exist in the physical spectrum as well as the standard-model-like Higgs h. Detailed study of the heavy Higgses provides information about some of the parameters in the MSSM like, for example, $\tan\beta$ [5–10]. Thus, the study of the heavy Higgses will be important for the study of the Higgs potential and electroweak symmetry breaking.

The study of the heavey Higgses is important both from the point of view of understanding electroweak symmetry breaking as well as for its deep impacts on cosmology. It has long been recognized that the dark matter in the universe, whose origin cannot be explained in the framework of the minimal standard model, may be explained in the MSSM. With the R-parity conservation, the lightest superparticle (LSP) is stable and hence, if its interaction is weak enough, LSP can be a viable candidate for the cold dark matter. Importantly, in a large fraction of the parameter space, the lightest neutralino becomes the LSP which can be the cold dark matter in this case. In the past, the relic density of the lightest neutralino has been intensively studied [11–19].

It should be noticed that, in order to realize the LSP dark matter, there is one caveat; in many cases, the thermal relic density of the LSP becomes larger than the currently measured dark-matter density. In particular, the density parameter of the dark matter is now well constrained by the Wilkinson microwave anisotropy probe (WMAP) [20,21]

$$\Omega_c^{(\mathrm{WMAP})} h^2 = 0.113^{+0.008}_{-0.009}, \tag{1.1}$$

and it is not automatic to realize such a density parameter with the LSP. It is often the case that some mechanism is needed to enhance the annihilation of the LSP to realize the LSP dark matter. Detailed study shows that the relic density of the LSP can become consistent with the WMAP value with some particular annihilation processes. In the so-called mSUGRA models, the parameter regions where the density parameter of the LSP becomes consistent with the WMAP value are classified as ''bulk region,'' ''coannihilation region,'' ''focus-point region,'' and ''rapid-annihilation funnels,'' although the annihilation mechanisms used in those regions work in a more general framework.

Once the supersymmetry is discovered, one of the challenges will be to determine the thermal relic density of the LSP and to see if the LSP dark matter is plausible [22–29]. If successful, it will give us deeper understandings of our universe up to the temperature of O(10 GeV). For this purpose, it is necessary to measure various parameters in the MSSM for the calculation of the thermal relic density of the LSP. Such studies have been also performed for the case of the LHC [16,30–34]. Most of those studies have, however, assumed a very simple model of supersymmetry breaking, like the mSUGRA model, in estimating the expected uncertainties in the reconstructed value of the thermal relic density of the LSP. We believe that, once the superparticles are found, it is necessary to calculate the

relic density in a model-independent way. Only with the LHC, such a study seems difficult in many cases.

With the ILC, on the contrary, precise determination of the MSSM parameters will be possible without assuming any particular model of SUSY breaking. Thus, in this case, the ILC will be able to help reconstructing the relic density of the LSP in many cases. For example, in the focus-point case, in [26], it was shown that the ILC can provide useful and significant information for the calculation of the thermal relic density of the LSP.

Here, we pay particular attention to another case, the rapid-annihilation funnels. In this case, pair annihilation of the LSP is dominated by the diagram with the s-channel exchange of the CP-odd neutral Higgs boson. In particular, in order to enhance the pair annihilation of the lightest neutralino, the $\tan\beta$ parameter becomes large in this case. If the LSP dark matter is realized in the rapid-annihilation funnels, detailed study of the heavy Higgs sector in the large $\tan\beta$ case is necessary to calculate the annihilation cross section of the LSP.

Strongly motivated by the dark-matter physics in the rapid-annihilation funnels (as well as the study of the Higgs potential), in this paper, we consider the strategy for studying the properties of the heavy Higgs bosons at the ILC assuming an energy and integrated luminosity of $\sqrt{s} = 1$ TeV and $L = 1$ ab^{-1}. We concentrate on the case where the $\tan\beta$ parameter is large and see how well we can constrain the properties of the heavy Higgs bosons. As we will discuss in the following sections, interactions of the heavy Higgses are well parameterized by five parameters. Using pair production processes of the neutral and charged Higgs bosons, these parameters can be constrained. If information from the neutral and charged Higgs production processes is combined, it will help in improving the determination of properties of the heavy Higgses. In this paper, we particularly consider how to combine information from various processes and how well the resultant constraint can be, using systematic consideration of the production and decay processes. Then, we also study how the results can be used to reconstruct the thermal relic density of the LSP.

The organization of this paper is as follows. In Sec. II, we briefly review the properties of the heavy Higgs bosons. In Sec. III, we discuss how and how well we can study the properties of the heavy Higgses at the ILC. In particular, we estimate the expected errors in the observed values of masses and widths of the heavy Higgses. Then, in Sec. IV, we discuss the implication of the ILC study of the heavy Higgses to the reconstruction of the dark-matter density. Section V is devoted to the conclusions and discussion.

II. HIGGS SECTOR

We start by discussing the Higgs bosons in the MSSM and by summarizing the relevant parameters for our analysis. As we mentioned, the MSSM contains two Higgs bosons H_u $(\mathbf{1}, \mathbf{2}, \frac{1}{2})$ and H_d $(\mathbf{1}, \mathbf{2}^*, -\frac{1}{2})$, where we have shown their quantum numbers of $SU(3)_C \times SU(2)_L \times U(1)_Y$ gauge group in the parenthesis. Both of these Higgs bosons acquire vacuum expectation values, which are parameterized by

$$\langle H_u^0 \rangle = v \sin\beta, \qquad \langle H_d^0 \rangle = v \cos\beta, \tag{2.1}$$

where $v \simeq 174$ GeV, and the angle β is a free parameter. After the electroweak symmetry breaking, it is usually the case that one linear combination of H_u and H_d becomes the standard-model-like Higgs $\Phi_{\rm SM}$ while the other combination Φ contains physical heavy Higgs, which are given by[1]

$$\begin{pmatrix} \Phi_{\rm SM} \\ \Phi \end{pmatrix} = \begin{pmatrix} \cos\beta & \sin\beta \\ -\sin\beta & \cos\beta \end{pmatrix} \begin{pmatrix} H_d \\ H_u^* \end{pmatrix}. \tag{2.2}$$

Using the mass eigenstates H, A, and $H^\pm$, the heavy Higgs doublet $\Phi = (\Phi^0, \Phi^-)$ is expressed as

$$\Phi^0 = \frac{1}{\sqrt{2}}(H + iA), \qquad \Phi^\pm = H^\pm. \tag{2.3}$$

In general two Higgs models, masses of H, A, and $H^\pm$ are unconstrained. In the MSSM, however, their masses, m_H, m_A, and $m_{H^\pm}$, are quite degenerate within a few GeV or so. For the neutral Higgs sector, this fact makes the study difficult. In our following study, we do not adopt the theoretical relation among these masses but we consider how well we can determine these three masses (in particular, m_H and m_A) at the ILC.

The productions of the heavy Higgses at the ILC are dominated by the gauge-boson exchange diagrams. In Fig. 1, we show the cross section for the processes $e^+e^- \to AH$ and $e^+e^- \to H^+H^-$ for several cases. (We will give the formula for the cross section in the following section; see Eqs. (3.5) and (3.19).) Here and hereafter, in our numerical study, we assume unpolarized electron beam.

Decay processes of the heavy Higgses have more model-dependence. In the rapid-annihilation funnels, heavy Higgses mostly decay into the third-generation quarks and leptons. We write the relevant interaction as[2]

$$\mathcal{L}_{\rm Yukawa} = y_b \Phi Q_3 b_R^c + y_t \Phi^* i\sigma^2 Q_3 t_R^c + y_\tau \Phi L_3 \tau_R^c + \text{h.c.}, \tag{2.4}$$

where Q_3 $(\mathbf{3}, \mathbf{2}, \frac{1}{6})$, b_R^c $(\mathbf{3}^*, \mathbf{1}, \frac{1}{3})$, t_R^c $(\mathbf{3}^*, \mathbf{1}, -\frac{2}{3})$, L_3 $(\mathbf{1}, \mathbf{2}, -\frac{1}{2})$, and τ_R^c $(\mathbf{1}, \mathbf{1}, 1)$ are third-generation quarks and leptons. In the parameter region we are interested in, the (fundamen-

[1]Strictly speaking, mixing in the CP-even neutral Higgs sector differs from those of other Higgses, and conventionally the mixing in the CP-even neutral Higgses are parameterized by the parameter α [35]. When the heavy Higgses are much heavier than the lightest Higgs (i.e., in the so-called ''decoupling limit''), however, it is expected that $\sin(\beta - \alpha) \to 1$ and Eq. (2.2) holds with good accuracy. In this paper, we only consider such a case.

[2]Notice that the Yukawa coupling constants y_b, y_t, and y_τ are different from those in the superpotential.

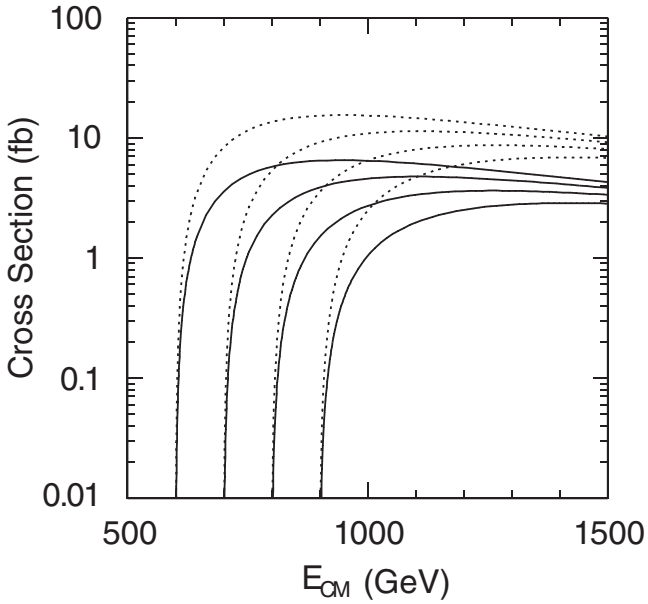

FIG. 1. Total cross sections for the heavy Higgs production processes as functions of the center of mass energy $E_{\rm CM} = \sqrt{s}$. The solid lines are for the process $e^+e^- \to AH$ with $m_A = m_H = 300$ GeV, 350 GeV, 400 GeV, and 450 GeV from above, while the dotted lines are for $e^+e^- \to H^+H^-$ with $m_{H^\pm} =$ 300 GeV, 350 GeV, 400 GeV, and 450 GeV from above.

tal) Yukawa coupling constants in the superpotential are fairly large. So, we expect that the radiative corrections do not significantly affect the relations between those with Yukawa coupling constants of the heavy Higgses. If we try to extract the information about these Yukawa coupling constants from the observed fermion masses, however, radiative correction may become important. At the tree level, the Yukawa coupling constants are related to the masses of the bottom quark, top quark and τ as

$$y_b^{(\rm tree)} = \frac{m_b \tan\beta}{v}, \qquad y_t^{(\rm tree)} = \frac{m_t \cot\beta}{v}, \qquad y_\tau^{(\rm tree)} = \frac{m_\tau \tan\beta}{v}. \tag{2.5}$$

Thus, once the "bottom-quark mass" m_b is well determined by the study of, for example, the lightest Higgs boson h, then the Yukawa coupling constant for τ can be also well determined at the tree level. It has been pointed out, however, that y_b receives sizable radiative correction from supersymmetric loop diagrams, in particular, at the large $\tan\beta$ region [36,37]. Thus, in determining the interaction of the heavy Higgses, it is dangerous to adopt the tree level relations.

In our analysis, we assume that several qualitative features of the large $\tan\beta$ region hold;, in particular, we consider the case where the heavy Higgses decay into third-generation quarks and leptons because of large y_b and y_τ. We do not, however, rely on the tree level relations among these Yukawa coupling constants but regard all the Yukawa couplings (in particular, y_b and y_τ) to be free parameters which should be experimentally determined.

In the large $\tan\beta$ region, y_t is extremely suppressed and, hereafter, we neglect its effects. Then, the neutral Higgses A and H decay mostly into the $b\bar{b}$ or $\tau\bar{\tau}$ final states.[3] The decay rates of the heavy Higgses are given by

$$\Gamma_{A\to b\bar{b}} = \frac{N_{\rm c}}{16\pi} y_b^2 m_A (1 + \Delta_{bb}^{(\rm QCD)}), \tag{2.6}$$

$$\Gamma_{A\to \tau\bar{\tau}} = \frac{1}{16\pi} y_\tau^2 m_A, \tag{2.7}$$

$$\Gamma_{H\to b\bar{b}} = \frac{N_{\rm c}}{16\pi} y_b^2 m_H (1 + \Delta_{bb}^{(\rm QCD)}), \tag{2.8}$$

$$\Gamma_{H\to \tau\bar{\tau}} = \frac{1}{16\pi} y_\tau^2 m_H, \tag{2.9}$$

$$\Gamma_{H^\pm\to bt} = \frac{N_{\rm c}}{16\pi} y_b^2 m_{H^\pm} \left(1 - \frac{m_t^2}{m_{H^\pm}^2}\right)^2 (1 + \Delta_{bt}^{(\rm QCD)}), \tag{2.10}$$

$$\Gamma_{H^\pm\to \tau\nu_\tau} = \frac{1}{16\pi} y_\tau^2 m_{H^\pm}, \tag{2.11}$$

where $N_{\rm c} = 3$ is the color factor and we neglect the masses of the fermions other than the top quark. Here, we denote the QCD corrections to the individual decay processes as $\Delta_{bb}^{(\rm QCD)}$ and $\Delta_{bt}^{(\rm QCD)}$. Importantly, the QCD corrections are calculable once the Higgs masses are determined [38,39]. Thus, if we can measure the decay widths and branching ratios of the heavy Higgses, we can constrain the Yukawa coupling constants. In addition, the total decay width of the heavy Higgses is given by

$$\Gamma_A = \Gamma_{A\to b\bar{b}} + \Gamma_{A\to \tau\bar{\tau}}, \tag{2.12}$$

$$\Gamma_H = \Gamma_{H\to b\bar{b}} + \Gamma_{H\to \tau\bar{\tau}}, \tag{2.13}$$

$$\Gamma_{H^\pm} = \Gamma_{H^\pm\to bt} + \Gamma_{H^\pm\to \tau\nu_\tau}. \tag{2.14}$$

As we will see below, in the rapid-annihilation funnels, decay widths of heavy Higgses are relatively large. Thus, from the invariant-mass distribution of the decay products, the decay widths may be measured at the ILC.

In summary, for the study of the heavy Higgs sector in the large $\tan\beta$ region, there are five relevant parameters so far: three masses m_A, m_H, $m_{H^\pm}$, and two Yukawa coupling constants y_b and y_τ. As we will see, the relic density of the LSP can be also well calculated in the rapid-annihilation funnels once these parameters are fixed. In the following, we will discuss how well these parameters are experimentally determined.

[3] H may also decay into the gauge boson or Higgs boson pair, but those processes are extremely suppressed in the large $\tan\beta$ region that we are interested in.

TABLE I. Underlying parameters to be used in our study.

	Point 1	Point 2
m_0	465.0 GeV	418.0 GeV
$m_{1/2}$	362.0 GeV	279.0 GeV
A_0	60.0 GeV	−12.0 GeV
$\tan\beta$	50	48
μ_H	444.5 GeV	357.7 GeV
m_A	400.0 GeV	350.0 GeV
m_H	401.4 GeV	351.0 GeV
$m_{H^\pm}$	412.9 GeV	363.6 GeV
Γ_A	20.7 GeV	17.1 GeV
$\Gamma_{H^\pm}$	19.7 GeV	14.9 GeV
$B_{A\to b\bar{b}}$	0.896	0.885
$m_{\chi_1^0}$	144.4 GeV	109.6 GeV
$m_{\chi_2^0}$	277.3 GeV	208.3 GeV
$m_{\chi_3^0}$	450.4 GeV	364.8 GeV
$m_{\chi_4^0}$	467.0 GeV	383.0 GeV
$m_{\chi_1^\pm}$	277.8 GeV	208.7 GeV
$m_{\chi_2^\pm}$	467.2 GeV	383.3 GeV
$\Omega_{\rm LSP}h^2$	0.113	0.113

Although our method can be applied to various cases, the whole parameter space is too large to be studied. Thus, we choose several parameter points and see how well we can experimentally measure parameters at the ILC in those cases. For simplicity, we generate the mass spectrum of the MSSM particles by adopting the mSUGRA boundary condition which is parameterized by the following parameters: universal scalar mass m_0, unified gaugino mass $m_{1/2}$, trilinear coupling coefficient A_0, $\tan\beta$, and the sign of the SUSY invariant Higgs mass sign(μ_H). Although we adopt the mSUGRA model as the underlying theory to fix the mass spectrum and mixing parameters, we consider a procedure to experimentally measure the parameters without assuming the mSUGRA. Since we are interested in the implication of such analysis for the study of the dark-matter physics, we adopt underlying parameters in the rapid-annihilation funnels. In Table I, we list the underlying parameters which we use. (We also show the density parameter of the LSP $\Omega_{\rm LSP}$ with those underlying parameters.)

III. HEAVY HIGGSES AT THE ILC

A. Outline

Now we discuss the study of the properties of the heavy Higgs bosons at the ILC. In particular, we are primarily interested in how and how well we can constrain the five parameters listed in the previous section by combining the information from the neutral and charged Higgs production processes. For this purpose, we adopt several reasonable approximations to simplify our analysis as we explain below, instead of studying the details of individual production and decay processes.

As we mentioned in the previous section, decay rates of the heavy Higgses are sensitive to the Yukawa coupling constants. Thus our strategy is to study branching ratios and the energy distribution of the final-state fermions produced by the decay of the heavy Higgses. Since the (total) decay rates are much smaller than the masses of the heavy Higgses, we can also measure the masses of the heavy Higgses from the energy distributions of the decay products.

Since we will try to determine the decay rates from the energy distribution of the final-state particles, we do not use the narrow width approximation for the heavy Higgs production cross section. In our analysis, the following type of the processes play a significant role: $e^+e^- \to \varphi_1^*\varphi_2^* \to f_1\bar{f}_1' f_2\bar{f}_2'$ where, in our case, (φ_1, φ_2) is (A, H) or (H^+, H^-) and f's are quarks and leptons. Let us denote the invariant-mass squared of the $f_i\bar{f}_i'$ system as $s_{f_i\bar{f}_i'}$. Then, for the processes we are interested in, the differential cross sections are well approximated by the following formula[4]

$$\frac{d\sigma(s)}{ds_{f_1\bar{f}_1'}ds_{f_2\bar{f}_2'}} = \frac{\hat{\sigma}(s; s_{f_1\bar{f}_1'}, s_{f_2\bar{f}_2'})}{\pi^2} \frac{s_{f_1\bar{f}_1'}^{1/2}\hat{\Gamma}_{\varphi_1\to f_1\bar{f}_1'}(s_{f_1\bar{f}_1'}^{1/2})}{(s_{f_1\bar{f}_1'} - m_{\varphi_1}^2)^2 + \Gamma_{\varphi_1}^2 m_{\varphi_1}^2} \times \frac{s_{f_2\bar{f}_2'}^{1/2}\hat{\Gamma}_{\varphi_2\to f_2\bar{f}_2'}(s_{f_2\bar{f}_2'}^{1/2})}{(s_{f_2\bar{f}_2'} - m_{\varphi_2}^2)^2 + \Gamma_{\varphi_2}^2 m_{\varphi_2}^2} + (\varphi_1 \leftrightarrow \varphi_2), \tag{3.1}$$

where the second term should be omitted if f_1 and f_2 are identical. Here, $\hat{\sigma}(s; s_{f_1\bar{f}_1'}, s_{f_2\bar{f}_2'})$ is the cross section for the process $e^+e^- \to \varphi_1^*\varphi_2^*$ with the masses of φ_1^* and φ_2^* being set equal to $s_{f_1\bar{f}_1'}^{1/2}$ and $s_{f_2\bar{f}_2'}^{1/2}$, respectively. In addition, $\hat{\Gamma}_{\varphi_i\to f_i\bar{f}_i'}(s_{f_i\bar{f}_i'}^{1/2})$ denotes the decay rate of φ_i^* whose mass is identified as $s_{f_i\bar{f}_i'}^{1/2}$; $\hat{\Gamma}_{\varphi_i\to f_i\bar{f}_i'}(s_{f_i\bar{f}_i'}^{1/2})$ can be obtained from Eqs. (2.6), (2.7), (2.8), (2.9), (2.10), and (2.11) by replacing the physical mass of the Higgs by $s_{f_i\bar{f}_i'}^{1/2}$. Explicit formulae of $\hat{\sigma}$ will be given in the following subsections. Notice that, when $\Gamma_{\varphi_i} \ll m_{\varphi_i}$, the total cross section becomes

$$\int ds_{f_1\bar{f}_1'}ds_{f_2\bar{f}_2'} \frac{d\sigma}{ds_{f_1\bar{f}_1'}ds_{f_2\bar{f}_2'}} \simeq (B_{\varphi_1\to f_1\bar{f}_1'}B_{\varphi_2\to f_2\bar{f}_2'} + B_{\varphi_2\to f_1\bar{f}_1'}B_{\varphi_1\to f_2\bar{f}_2'}) \times \sigma_{e^+e^-\to\varphi_1\varphi_2}, \tag{3.2}$$

[4]For the process we consider (i.e., $e^+e^- \to f_1\bar{f}_1' f_2\bar{f}_2'$), there are in fact several diagrams where some of the fermions are not emitted from the virtual Higgs bosons (like $e^+e^- \to f_1^*\bar{f}_1'$, followed by $f_1^* \to f_1 + \varphi^*$ and $\varphi^* \to f_2\bar{f}_2'$). In the parameter region where $s_{f_1\bar{f}_1'}^{1/2}$ and $s_{f_2\bar{f}_2'}^{1/2}$ are both close to the Higgs mass(es), however, we have checked that the cross section is dominated by the process $e^+e^- \to \varphi_1^*\varphi_2^* \to f_1\bar{f}_1' f_2\bar{f}_2'$. Thus, we use Eq. (3.1) for simplicity.

where

$$\sigma_{e^+e^-\to\varphi_1\varphi_2}(s) = \hat{\sigma}(s; m^2_{\varphi_1}, m^2_{\varphi_2}). \tag{3.3}$$

As suggested by Eq. (3.1), the distributions of the invariant masses of the final-state fermions have peaks around $s^{1/2}_{f_i\bar{f}'_i} \sim m_{\varphi_i}$. In addition, the distributions become broader as the decay rate Γ_{φ_i} becomes larger. Thus, in the heavy Higgs production processes, the invariant-mass distributions of the final-state fermions have important information about the masses and the decay widths of the heavy Higgses.

It should be, however noted that the observed invariant-mass distributions are deformed by several effects. One reason is the energy loss by the neutrino emission. With the leptonic decays, some fraction of the initial energy of the bottom quark may be carried away by energetic neutrinos and the energy of the b-jet becomes underestimated. Another important effect is from the resolution of the calorimeters (in particular, the hadronic calorimeter). In order to simulate these effects, we perform a Monte Carlo (MC) analysis. Here, we first generate parton-level events for a given value of the collider energy $\sqrt{s}$, which we take to be 1 TeV throughout this paper unless otherwise mentioned. In each event, in general, momenta of bottom quarks $p^{(0)}_{b_i}$, other lighter quarks $p^{(0)}_{q_i}$, and leptons $p^{(0)}_{l_i}$ are generated. If the final-state partons contain the top quark, its decay (as well as the subsequent decay of $W^{\pm}$) is also taken into account at this state. Here and hereafter, the superscript (0) is for momenta of the primary partons before the hadronization and cascade decay. In order to consider the energy loss of the bottom quark in the leptonic decay events, we used ISAJET package [40] to follow the hadronization and decay chain of the bottom quark. For individual primary bottom quark with (initial) momentum $p^{(0)}_{b_i}$, we calculate the fraction of the visible energy f_{b_i} after its hadronization and decay. Then, the b-jet (after the hadronization and the decay) is treated as the jet with the momentum $f_{b_i}p^{(0)}_{b_i}$. In addition, because of the detector resolution, distribution of the observed energy of the jet is smeared. In order to determine the observed momentum of the individual jets, we adopt the energy resolution of the hadronic calorimeter to be $\sigma_{\rm E}/E = 40\%/\sqrt{E}$ (with E being the energy of the jet) [1,41]. As a result, with the generated momenta of the quarks $p^{(0)}_{b_i}$ and $p^{(0)}_{q_i}$, we determine the observed energy p_{b_i} and p_{q_i}. (We also denote corresponding observed energy as E_{b_i} and E_{q_i}.)

B. Neutral Higgs production

Let us first consider the neutral Higgs production $e^+e^- \to AH$. In the large $\tan\beta$ region, A and H both dominantly decay into $b\bar{b}$ and $\tau\bar{\tau}$. Thus, there are three types of final states:[5]

$$e^+e^- \to A^*H^* \to \begin{cases} bbbb \\ bb\tau\tau. \\ \tau\tau\tau \end{cases} \tag{3.4}$$

The cross section for the process $e^+e^-_{L,R} \to A^*H^*$ is given by

$$\hat{\sigma}_{e^+e^-_{L,R}\to A^*H^*}(s, m^2_{A^*}, m^2_{H^*}) = \frac{sv^3_{AH}}{192\pi}\frac{f^2_{L,R}g^2_z}{(s-m^2_Z)^2}\sin^2(\beta-\alpha), \tag{3.5}$$

where $g_Z \equiv \sqrt{g^2_1 + g^2_2}$ with g_1 and g_2 being gauge coupling constants for the $U(1)_Y$ and $SU(2)_L$ gauge groups, respectively, m_Z is the Z-boson mass, α is the mixing angle in the CP-even Higgs sector,

$$v^2_{AH} = \frac{1}{s}[(s - m^2_{A^*} - m^2_{H^*})^2 - 4m^2_{A^*}m^2_{H^*}], \tag{3.6}$$

and, for the left- and right-polarized electron beam,

$$f_L = \frac{g^2_2 - g^2_1}{g_z}, \qquad f_R = -\frac{g^2_1}{g_z}. \tag{3.7}$$

We take $\sin^2(\beta-\alpha) = 1$ since we are interested in the limit where the heavy Higgses are much heavier than the lightest Higgs.

In our analysis, we use the first two types of events: $bbbb$ ($4b$) final state and $bb\tau\tau$ final state. We do not consider $\tau\tau\tau\tau$ final state because the branching ratios of the heavy neutral Higgses into the $\tau\tau$ final state are fairly small (~ 0.1) so the number of 4τ events is suppressed.

The branching ratios $B_{A\to b\bar{b}}$ and $B_{H\to b\bar{b}}$ are $\sim$0.9 so sizable number of $4b$ event is expected. At the ILC, such an event will be identified by the following features:

(a) 4 b-tagged jets.
(b) Small missing energy.
(c) No isolated leptons.

Once observed, the distribution of the invariant mass of two b-jets provides important information about the properties of the heavy Higgs bosons. Energy and invariant-mass distributions of the primary partons are relatively easily calculated. As we mentioned in the previous subsection, however, observed distributions are different from the primary ones because of the leptonic decay of the bottom quark and also because of the resolution of the calorimeters. We are particularly interested in the distribution of the invariant mass of two b-jets which originate from (virtual) neutral Higgs bosons. In order to pair the b-jets, we use the fact that the masses of the two (heavy) neutral Higgses are expected to be quite degenerate. Consequently, the total energy of $b\bar{b}$ system from the

[5]For simplicity, sometimes we do not distinguish particle and antiparticle when there is no confusion.

virtual A becomes very close to that from the virtual H. Thus, for the event $e^+e^- \to b_1 b_1' b_2 b_2'$ (where the b-jets are ordered so that the observed energy be $E_{b_1} < E_{b_2} < E_{b_2'} < E_{b_1'}$), we define the following two invariant masses:

$$m_{bb,1}^2 = (p_{b_1} + p_{b_1'})^2, \qquad m_{bb,2}^2 = (p_{b_2} + p_{b_2'})^2. \quad (3.8)$$

In general, we can perform statistical analysis based on the distributions of these two invariant masses. For simplicity, however, we use ''averaged'' distribution

$$\frac{dN_{4b}}{dm_{bb}} \equiv \frac{1}{2}\int dm_{bb,1}\left[\frac{dN_{4b}}{dm_{bb,1}dm_{bb,2}}\right]_{m_{bb,2}=m_{bb}} + \frac{1}{2}\int dm_{bb,2}\left[\frac{dN_{4b}}{dm_{bb,1}dm_{bb,2}}\right]_{m_{bb,1}=m_{bb}}, \quad (3.9)$$

where N_{4b} is the number of $4b$ events. As we will see, even from this averaged distribution, we obtain significant constraints on the masses and decay rates of the neutral Higgses.

In order to determine the distribution given in Eq. (3.9), we calculate the ''transfer functions'' for the $4b$ events $T_{4b}(m_{bb}; s_{b_1\bar{b}_1}, s_{b_2\bar{b}_2})$; T_{4b} is the distribution of the observable m_{bb} for the event with $s_{b_1\bar{b}_1}$ and $s_{b_2\bar{b}_2}$ being fixed. In calculating the transfer function, several kinematical constraints are taken into account to eliminate standard-model backgrounds. In the $4b$ events, all the beam energy is carried away by the bottom quarks. In addition, for the process $e^+e^- \to A^*H^*$ followed by $A^* \to b_1\bar{b}_1$ and $H^* \to b_2\bar{b}_2$, $E_{b_1} + E_{\bar{b}_1}$ becomes close to $E_{b_2} + E_{\bar{b}_2}$ in most of the cases. The kinematical cuts based on these can be used to eliminate some of the backgrounds; here, for the event $e^+e^- \to b_1 b_1' b_2 b_2'$ with $E_{b_1} < E_{b_2} < E_{b_2'} < E_{b_1'}$, we adopt

(a) 960 GeV $\le E_{b_1} + E_{b_1'} + E_{b_2} + E_{b_2'} \le$ 1040 GeV.
(b) 470 GeV $\le E_{b_1} + E_{b_1'} \le$ 530 GeV and 470 GeV $\le E_{b_2} + E_{b_2'} \le$ 530 GeV.
(c) There is no leptonic activity (with energy greater than 25 GeV), in particular, in the b-jets.
(d) Invariant masses of any two of the jets are larger than 130 GeV.

With the excellent b-tagging capability of the ILC, we expect that significant fraction of the b-jets can be identified. Tagging of all four bottom quarks will help eliminating standard-model backgrounds. Using the transfer function, we obtain

$$\frac{dN_{4b}}{dm_{bb}} = \epsilon_b^4 L \int ds_{b_1\bar{b}_1} ds_{b_2\bar{b}_2} T_{4b}(m_{bb}; s_{b_1\bar{b}_1}, s_{b_2\bar{b}_2}) \times \frac{d\sigma_{e^+e^-\to A^*H^*\to b\bar{b}b\bar{b}}}{ds_{b_1\bar{b}_1} ds_{b_2\bar{b}_2}}, \quad (3.10)$$

with L being the luminosity. Here, ϵ_b is the tagging efficiency of single bottom quark; we approximate that the b-tagging efficiency is independent of the number of b-jets and take $\epsilon_b = 0.7$ in our numerical calculations [1–3]. Then, in the statistical analysis, we calculate the number of $4b$ events integrated over some intervals of the invariant mass:

$$N_{4b}^{(i)} = \int_{m_{bb}^{(i)}}^{m_{bb}^{(i+1)}} dm_{bb} \frac{dN_{4b}}{dm_{bb}}, \quad (3.11)$$

where $m_{bb}^{(i)}$ and $m_{bb}^{(i+1)}$ are lower and upper bounds of the i-th bin.

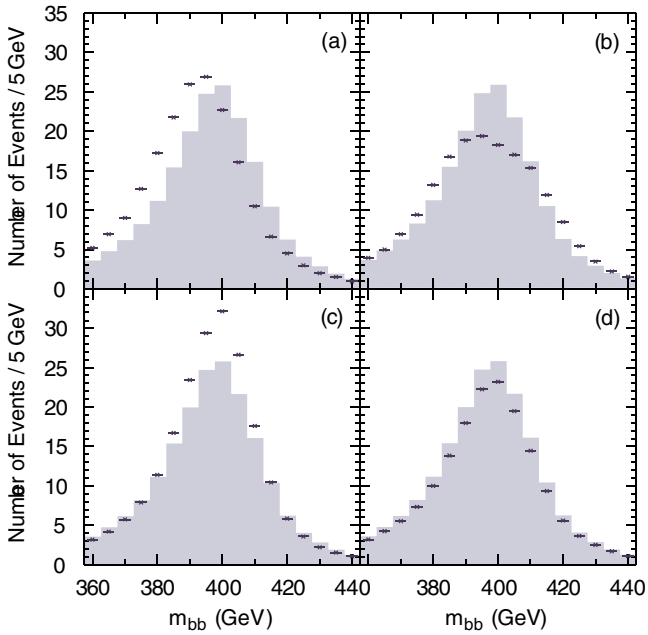

FIG. 2 (color online). Number of $4b$ events in each bin (with the width of 5 GeV) with $L = 1$ ab^{-1}. The histogram shows the result for the point 1: $\bar{m}_{AH} = 400.7$ GeV, $\Delta m_{AH} = -0.7$ GeV, $\Gamma_A = 20.7$ GeV, and $B_{A\to b\bar{b}} = 0.896$. The short horizontal lines with ''$\times$'' are those with one of the four parameters being changed: (a) $\bar{m}_{AH} = 395$ GeV, (b) $\Delta m_{AH} = 10$ GeV, (c) $\Gamma_H = 15$ GeV, and (d) $B_{A\to b\bar{b}} = 0.85$.

Although we imposed several kinematical cuts, there may still remain backgrounds. Since we required that the total energy of the final-state jets is close to $\sqrt{s}$ as well as that $4b$-tagged jets exist, we suppose that the dominant background is from the events of the type $e^+e^- \to b\bar{b}b\bar{b}$. We use COMPHEP package [42] to generate such events and, using the kinematical cuts we discussed before, we estimate the number of backgrounds. We found that, however, the number of background from the process $e^+e^- \to b\bar{b}b\bar{b}$ is negligibly small (~ 0.01 event/5 GeV/1 ab^{-1}). There may also exist another class of backgrounds which arise from the misidentification of the b-jet. Study of such background requires detailed study of the detector effects and we leave such a study for a future work.[6]

In Fig. 2, we show the number of events and backgrounds in each bin. Since A and H are quite degenerate,

[6]Invariant-mass distribution of the $4b$ event has been also studied in [22], where it is also shown that the background for the $4b$ event is well below the signal.

it is convenient to define the "averaged mass" and the "mass difference" as follows:

$$\bar{m}_{AH} \equiv \frac{1}{2}(m_A + m_H), \qquad \Delta m_{AH} \equiv \frac{1}{2}(m_A - m_H). \tag{3.12}$$

(We will see that error in $\bar{m}_{AH}$ is much smaller than that in Δm_{AH}.) As one can see, the distribution of m_{bb} is peaked at around $m_{bb} \sim \bar{m}_{AH}$. In addition, width and height of the distribution depend on the mass and decay parameters. Thus, from the observed distribution of m_{bb}, mass and decay width of the neutral Higgses will be determined.

Some fraction of the neutral Higgses also decay into $\tau\bar{\tau}$ pair, so we can also use the events with $b\bar{b}\tau\bar{\tau}$ final state. Here we only use the hadronic decay mode of τ to identify the τ jets; when the τ lepton decays hadronically, we obtain a jet with low multiplicity. Using this fact, we assume that the hadrons from τ can be well identified and distinguished from the jets from the direct production of quarks. Then, the $bb\tau\tau$ event is specified by the following features:

(a) $2b$-tagged jets (b and b') with the total energy of the system being close to $\frac{1}{2}\sqrt{s}$.
(b) 2 energetic isolated jets with low multiplicity.

Since, in the signal event, two b-jets originate from single (virtual) neutral Higgs, we use the distribution of the invariant mass of two b-jets to determine the masses and widths of the neutral Higgses:

$$m_{bb}^2 = (p_b + p_{b'})^2. \tag{3.13}$$

For the $bb\tau\tau$ event, we also calculate the transfer function $T_{bb\tau\tau}$ with MC simulation. Then, we obtain

$$\frac{dN_{bb\tau\tau}}{dm_{bb}} = \epsilon_b^2 L B_{\tau\to\text{had}}^2 \int ds_{b\bar{b}} ds_{\tau\bar{\tau}} T_{bb\tau\tau}(m_{bb}; s_{b_1\bar{b}_1}, s_{b_2\bar{b}_2}) \times \frac{d\sigma_{e^+e^-\to A^*H^*\to b\bar{b}\tau\bar{\tau}}}{ds_{b\bar{b}} ds_{\tau\bar{\tau}}}, \tag{3.14}$$

where $B_{\tau\to\text{had}} \simeq 0.65$ [21] is the hadronic branching ratio of τ. In calculating $T_{bb\tau\tau}$, we take account of the following kinematical cuts:

(a) 470 GeV $\le E_b + E_{b'} \le$ 530 GeV.
(b) In the b-jets, there is no leptonic activity with energy higher than 25 GeV.
(c) Angle between two jets from τ leptons is larger than $\frac{1}{2}\pi$.

For the $bb\tau\tau$ event, the $t\bar{t}$ production process provides irreducible background; $e^+e^- \to t\bar{t}$ followed by the τ-leptonic decay of both the $W^\pm$-bosons produced by the top decays. For this process, we generate the events and estimate the number of background of this type. We found that the number of events from this type of background is $(0.1 - 1)$ event/5 GeV/1 ab^{-1}, which is below the number of signal event. As well as from the $t\bar{t}$ production process, we may also have backgrounds from the four-body production process $e^+e^- \to b\bar{b}\tau\bar{\tau}$, which is also possible in the standard model. To see how large it is, we generate such event with COMPHEP package and estimated the number of background. We found that the number of such background events is very small after imposing the kinematical cuts, $\sim$0.01 events per each bin (with $L =$ 1 ab^{-1}) which is well below the number of signal event.

Invariant-mass distribution of the $bb\tau\tau$ event is shown in Fig. 3. As in the case of $4b$ event, the distribution is peaked at around the heavy neutral Higgs masses. The number of $bb\tau\tau$ event is, however, proportional to $B_{A\to b\bar{b}}(1 - B_{A\to b\bar{b}})$ and hence is suppressed compared to that of the $4b$ event. As a result, $4b$ event is statistically more important than $bb\tau\tau$ event.

Using the above results, we can estimate the expected errors in the measured values of the physical quantities. For this purpose, we first determine the underlying values of the fundamental parameters. For the neutral Higgs production processes, there are four free parameters; here we use m_A, m_H (or $\bar{m}_{AH}$, Δm_{AH}), Γ_A, and $B_{H\to b\bar{b}}$ as parameters to specify the point in the parameter space. We use the parameter sets given in Table I as underlying parameters unless otherwise stated. With the underlying parameters, we calculate the expected number of $4b$ and $bb\tau\tau$ events in each bin, which we denote $\bar{N}_{4b}^{(i)}$ and $\bar{N}_{bb\tau\tau}^{(i)}$. Then, in order to see how well the underlying values can be determined, we calculate the number of events in each bin, $N_{4b}^{(i)}$ and $N_{bb\tau\tau}^{(i)}$, for postulated values of m_A, m_H, Γ_A, and $B_{H\to b\bar{b}}$, and see if $\bar{N}_{4b}^{(i)}$ and $\bar{N}_{bb\tau\tau}^{(i)}$ are statistically consistent with $N_{4b}^{(i)}$ and $N_{bb\tau\tau}^{(i)}$. Here, we define the $\delta\chi^2$ variable for the neutral Higgs production as

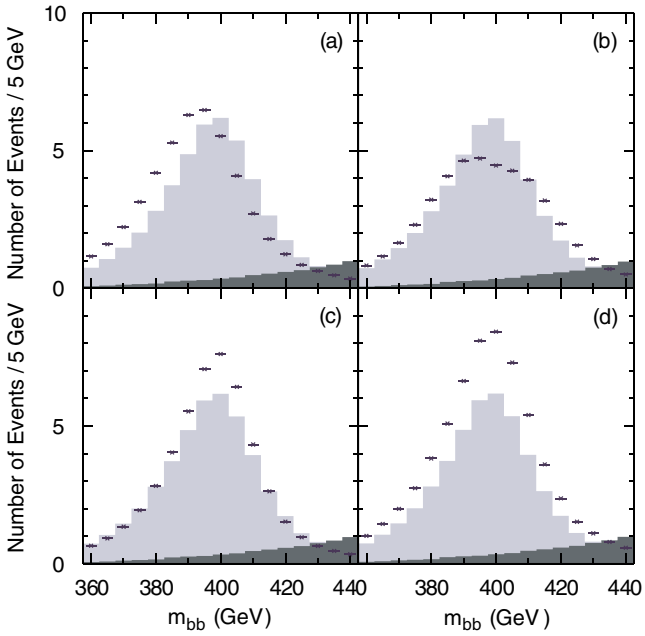

FIG. 3 (color online). Same as Fig. 2, but for the $bb\tau\tau$ events. The background from the $t\bar{t}$ production process is also shown in the darkly shaded histogram.

$$\delta\chi^2_{\rm N} = \sum_i \frac{(\bar{N}^{(i)}_{4b} - N^{(i)}_{4b})^2}{N^{(i)}_{4b} + N^{(i)}_{4b,\rm BG}} + \sum_i \frac{(\bar{N}^{(i)}_{bb\tau\tau} - N^{(i)}_{bb\tau\tau})^2}{N^{(i)}_{bb\tau\tau} + N^{(i)}_{bb\tau\tau,\rm BG}}, \quad (3.15)$$

where $N^{(i)}_{4b,\rm BG}$ and $N^{(i)}_{bb\tau\tau,\rm BG}$ are numbers of backgrounds for the $4b$ and $bb\tau\tau$ events, respectively.

With $\delta\chi^2_{\rm N}$, we estimate how well we can determine the physical quantities. Since $\delta\chi^2_{\rm N}$ depends on four independent parameters, we fix two of them and show the behaviors of $\delta\chi^2_{\rm N}$ on several two-dimensional hyperplanes. First, we consider the constraints on the masses of the neutral Higgses. For this purpose, we consider the hyperplane with Γ_A and $B_{A\to b\bar{b}}$ being fixed and show the contours of constant $\delta\chi^2_{\rm N}$ on Δm_{AH} vs $\bar{m}_{AH}$ plane. In Fig. 4, we show the results. In particular, in Fig. 4(a), we show the behavior of $\delta\chi^2_{\rm N}$ on the hyperplane with Γ_A and $B_{A\to b\bar{b}}$ being equal to their underlying values. As one can see, if we consider the contour of $\delta\chi^2_{\rm N} = 1$, error of $\bar{m}_{AH}$ is $\sim$1 GeV while that of Δm_{AH} is $\sim$6 GeV. We also show the contours of constant $\delta\chi^2_{\rm N}$ on other plane. We can see that the contours for $\delta\chi^2_{\rm N} = 2$ and 4 are almost unchanged while the region with $\delta\chi^2_{\rm N} < 1$ is reduced. From the fact that the error in $\bar{m}_{AH}$ is significantly smaller than that in Δm_{AH}, we expect that the error in the determination of the masses of heavy neutral Higgses is dominantly from that of Δm_{AH}.

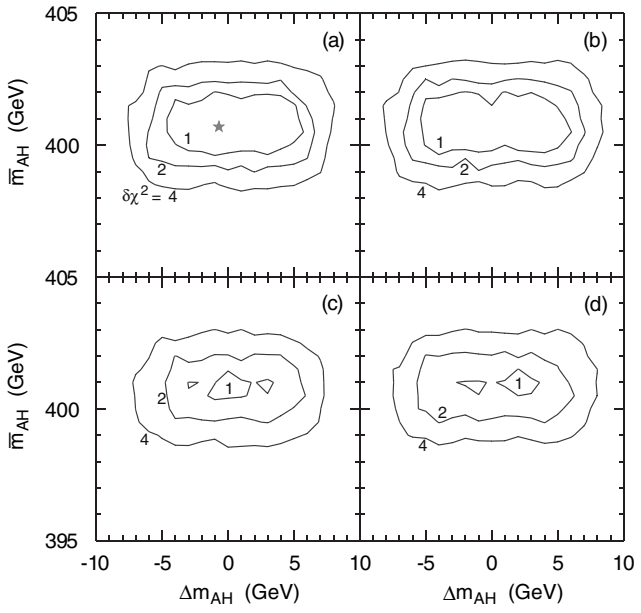

FIG. 4. Contours of constant $\delta\chi^2_{\rm N}$ on Δm_{AH} vs $\bar{m}_{AH}$ planes; $\delta\chi^2_{\rm N} = 1$, 2, and 4 (with $L = 1$ ab^{-1}) from inside and the "star" on the figure indicates the underlying point. As the underlying point, we take the point 1 in Table I. For the calculation of $N^{(i)}_{4b}$ and $N^{(i)}_{b\tau\tau\nu_\tau}$ in Eq. (3.15), we take Γ_A and $B_{A\to b\bar{b}}$ to be (a) $\Gamma_A = 20.7$ GeV and $B_{A\to b\bar{b}} = 0.896$ (underlying values), (b) $\Gamma_A = 19.7$ GeV and $B_{A\to b\bar{b}} = 0.896$, (c) $\Gamma_A = 20.7$ GeV, and $B_{A\to b\bar{b}} = 0.88$, (d) $\Gamma_A = 19.7$ GeV, and $B_{A\to b\bar{b}} = 0.88$.

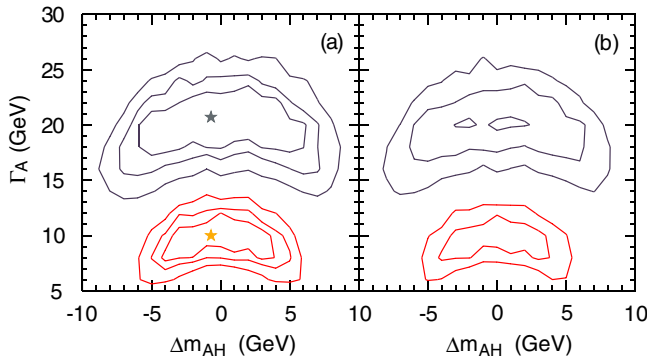

FIG. 5 (color online). Contours of constant $\delta\chi^2_{\rm N}$ on Δm_{AH} vs Γ_A planes; $\delta\chi^2_{\rm N} = 1$, 2, and 4 (with $L = 1$ ab^{-1}) from inside. We fix $\bar{m}_{AH}$ and $B_{A\to b\bar{b}}$ to be (a) $\bar{m}_{AH} = 400.7$ GeV and $B_{A\to b\bar{b}} = 0.896$ (the underlying values), and (b) $\bar{m}_{AH} = 400.7$ GeV and $B_{A\to b\bar{b}} = 0.88$. For the upper contours, the underlying values are given by the point 1. For the lower contours, the underlying value of Γ_A is taken to be 10 GeV. (In (b), there is no contour for $\delta\chi^2_{\rm N} = 1$ for the case of $\Gamma_A = 10$ GeV.)

Next, let us consider the uncertainties in other quantities. In Fig. 5, we show the contours of constant $\delta\chi^2_{\rm N}$ on the hyperplane of $\bar{m}_{AH}$ and $B_{A\to b\bar{b}}$ being fixed. From this figure, we can see that the uncertainty in Γ_A is 2–3 GeV when the underlying value is $\Gamma_A \simeq 20$ GeV. In fact, the uncertainties are sensitive to the underlying value of Γ_A. To see this, we also show the results for the case where the underlying value of Γ_A is 10 GeV (with other underlying parameters being unchanged). In this case, we can see that the errors in Δm_{AH} and Γ_A are reduced.

Using the $\delta\chi^2_{\rm N}$ variable, we can also constrain the branching ratios. In Fig. 6, we plot the contours of constant $\delta\chi^2_{\rm N}$ on $\Delta m_{\rm N}$ vs $B_{A\to b\bar{b}}$ plane. We can see that $B_{A\to b\bar{b}}$ can be constrained at the level of $\sim$5% and hence we can conclude that $B_{A\to b\bar{b}}$ can be well determined.

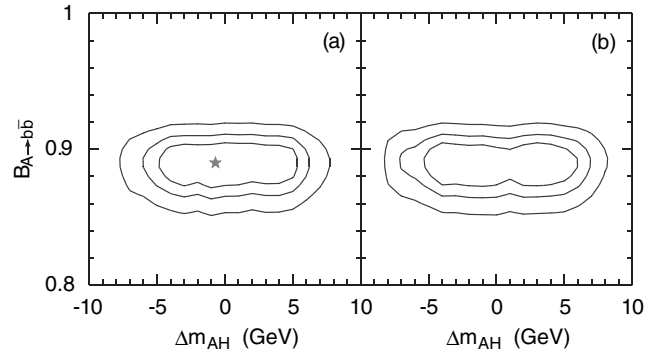

FIG. 6. Contours of constant $\delta\chi^2_{\rm N}$ for the point 1 on Δm_{AH} vs $B_{A\to b\bar{b}}$ planes; $\delta\chi^2_{\rm N} = 1$, 2, and 4 (with $L = 1$ ab^{-1}) from inside. Here, $\bar{m}_{AH}$ and Γ_A are fixed to be (a) $\bar{m}_{AH} = 0.7$ GeV, and $\Gamma_A = 20.7$ GeV (the underlying values), and (b) $\bar{m}_{AH} = 0.7$ GeV and $\Gamma_A = 19.7$ GeV.

C. Charged Higgs production

Next, we consider the charged Higgs events. The useful decay modes in the large $\tan\beta$ case are $H^\pm \to bt$ and $\tau\nu_\tau$. Thus, in the charged Higgs events, relevant final states are

$$e^+e^- \to H^{+*}H^{-*} \to \begin{cases} btbt \\ bt\tau\nu_\tau \\ \tau\nu_\tau\tau\nu_\tau \end{cases}. \tag{3.16}$$

We expect significant amount of irreducible backgrounds for the $\tau\nu_\tau\tau\nu_\tau$ event, in particular, from the W^+W^- production. Thus, we do not consider this mode.

First, we consider the $bt\tau\nu_\tau$ final state. After the decay of the top quark, we obtain $W^\pm$-boson and b. In order to determine the mass of the charged Higgs, we only use the hadronic decay of the $W^\pm$-boson. In addition, for τ, we again use only the hadronic decay mode to identify the τ-lepton events. Then, the relevant $bt\tau\nu_\tau$ event has the following features:

(a) $2b$-tagged jets (b_1 and b_2).
(b) 2 non-b-like jets (q_1 and q_2).
(c) 1 energetic isolated jet with low multiplicity.

To eliminate backgrounds, we also impose several kinematical constraints. Since the event is dominated by the back-to-back production of the charged Higgs bosons (which are almost on-shell), total energy of the bt system is close to $\frac{1}{2}\sqrt{s}$ in most of the signal events. In addition, if we consider the system consisting of q_1, q_2 and one of the b-jet, its invariant mass becomes close to m_t. (We may be able to use the fact that the invariant mass of the system consisting of q_1 and q_2 system is close to m_W although, in our numerical analysis, we do not take into account such constraint.)

In the $bt\tau\nu_\tau$ event, all the hadronic activities except the isolated hadrons from τ are from one of the charged Higgs, so the invariant mass of such system contain information about the mass and decay width of $H^\pm$. Thus, we define

$$m_{bt}^2 \equiv (p_{b_1} + p_{b_2} + p_{q_1} + p_{q_2})^2, \tag{3.17}$$

and calculate the distribution of m_{bt} by MC analysis. In deriving the distribution of this invariant mass, we impose the following cuts:

(a) 470 GeV $\le E_{b_1} + E_{b_2} + E_{q_1} + E_{q_2} \le$ 530 GeV.
(b) 150 GeV $\le m_{b_1q_1q_2} \le$ 200 GeV or 150 GeV $\le m_{b_2q_1q_2} \le$ 200 GeV, where $m_{b_iq_1q_2}^2 \equiv (p_{b_i} + p_{q_1} + p_{q_2})^2$.
(c) No leptonic activity (with energy larger than 25 GeV) in the b-jets.

Then, we calculate the transfer function $T_{bt\tau\nu_\tau}$ to estimate

$$\frac{dN_{bt\tau\nu_\tau}}{dm_{bt}} = \epsilon_b^2 LB_{\tau\to\mathrm{had}}B_{W^\pm\to q\bar{q}} \times \int ds_{bt}ds_{\tau\nu_\tau}T_{bt\tau\nu_\tau}(m_{bt}; s_{bt}, s_{\tau\nu_\tau}) \times \frac{d\sigma_{e^+e^-\to H^{+*}H^{-*}\to bt\tau\nu_\tau}}{ds_{bt}ds_{\tau\nu_\tau}}, \tag{3.18}$$

where $B_{W^\pm\to q\bar{q}} \simeq 0.676$ [21] is the branching ratio of the hadronic decay of $W^\pm$-boson. Here, the cross section for $e^+e^- \to H^{+*}H^{-*}$ is given by

$$\hat{\sigma}_{e^+e^-_{L,R}\to H^{+*}H^{-*}}(s; m_{H^{+*}}^2, m_{H^{-*}}^2) = \frac{sv_{H^\pm}^3}{48\pi}\left(\frac{e^2}{s} + f_{L,R}\frac{g_2^2 - g_1^2}{g_z}\frac{1}{s - m_Z^2}\right)^2, \tag{3.19}$$

where e is the electric charge, and $v_{H^\pm}$ is obtained from Eq. (3.6) by replacing $m_{A^*} \to m_{H^{+*}}$ and $m_{H^*} \to m_{H^{-*}}$.

In Fig. 7, we plot the distribution of the invariant mass m_{bt} for several cases. First of all, as one can see, the distribution function is peaked at around $\sim m_{H^\pm}$. In addition, the distribution becomes broader as the decay width $\Gamma_{H^\pm}$ becomes larger. Notice that the number of $bt\tau\nu_\tau$ event is approximately proportional to $B_{H^\pm\to bt}(1 - B_{H^\pm\to bt})$.

For the $bt\tau\nu_\tau$ process, there exists irreducible background from the $t\bar{t}$ pair production process, if one of the $W^\pm$ boson decays hadronically while the other decays into τ and ν_τ. We have estimated the number of the background from $t\bar{t}$ pair production, generating such events. The result is also shown in Fig. 7; the number of background is well below the number of signal event. We also calculated the background from the standard-model process of $e^+e^- \to bt\tau\nu_\tau$ with the COMPHEP package with eliminating the contribution from the process $e^+e^- \to t\bar{t}$; we found that the number of background event of this type is extremely small.

As a charged Higgs production event, $b\bar{t}\,\bar{b}\,t$ final-state event is also available. In this case, we expect four b-tagged jets and other hadronic and/or leptonic activities in the final state (from the decay of the $W^\pm$ bosons). In the $btbt$ events, however, the reconstruction of the invariant mass of the bt system of one side seems challenging because of the combination error or overlap of the jets (although it may be possible with some careful analysis).

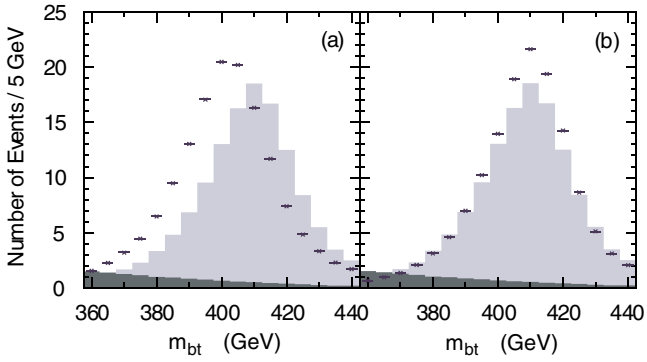

FIG. 7 (color online). Number of $bt\tau\nu_\tau$ events in each bin. The shaded histogram shows the result for the point 1: $m_{H^\pm} =$ 412.9 GeV, $\Gamma_{H^\pm} =$ 19.7 GeV, and $B_{H^\pm\to bt} = 0.885$. The short horizontal lines with "×" are those with one of the parameters being changed: (a) $m_{H^\pm} =$ 405 GeV, and (b) $\Gamma_{H^\pm} =$ 15 GeV. The background from the $t\bar{t}$ production process is also shown in the darkly shaded histogram.

Thus, in this paper, we only use the total number of the $btbt$ event to constrain the branching ratio, using the fact that the number of the $btbt$ event is approximately proportional to $B^2_{H^\pm\to bt}$. Here, we estimate the number of $btbt$ event as

$$N_{btbt} = \epsilon_b^4 B^2_{H^\pm\to bt} L \sigma_{e^+e^-\to H^+H^-}. \tag{3.20}$$

As in the case of the neutral Higgs, we calculate the $\delta\chi^2$ variable; for the $bt\tau\nu_\tau$ event, we calculate the number of events falling into each bin, which is classified by m_{bt}. The number of event in the i-th bin $N^{(i)}_{bt\tau\nu_\tau}$ is calculated as a function of independent parameters (in the charged Higgs case, $m_{H^\pm}$, $\Gamma_{H^\pm}$, and $B_{H^\pm\to bt}$). For the $btbt$ event, we use only the total number of events N_{btbt}. Then, we define

$$\delta\chi^2_{\rm C} = \sum_i \frac{(\bar{N}^{(i)}_{bt\tau\nu_\tau} - N^{(i)}_{bt\tau\nu_\tau})^2}{N^{(i)}_{bt\tau\nu_\tau} + N^{(i)}_{bt\tau\nu_\tau,{\rm BG}}} + \frac{(\bar{N}_{btbt} - N_{btbt})^2}{N_{btbt} + N_{btbt,{\rm BG}}}, \tag{3.21}$$

where the second terms in the denominators are the numbers of background events.

In Fig. 8, we show the contours of constant $\delta\chi^2_{\rm C}$ on $m_{H^\pm}$ vs $\Gamma_{H^\pm}$ planes. We can see that, from the contour of $\delta\chi^2_{\rm C} = 1$, the uncertainty in $m_{H^\pm}$ is 1–2 GeV while that in $\Gamma_{H^\pm}$ is $\sim$3 GeV. We can also see that the inclusion of the $tbtb$ mode can help reducing the allowed region on the $m_{H^\pm}$ vs $\Gamma_{H^\pm}$ plane. In Fig. 9, we also show the contours of constant $\delta\chi^2_{\rm C}$ on $m_{H^\pm}$ vs $B_{H^\pm\to bt}$ planes. We can see that the branching ratio $B_{H^\pm\to bt}$ is also well constrained by the study of the charged Higgs production processes.

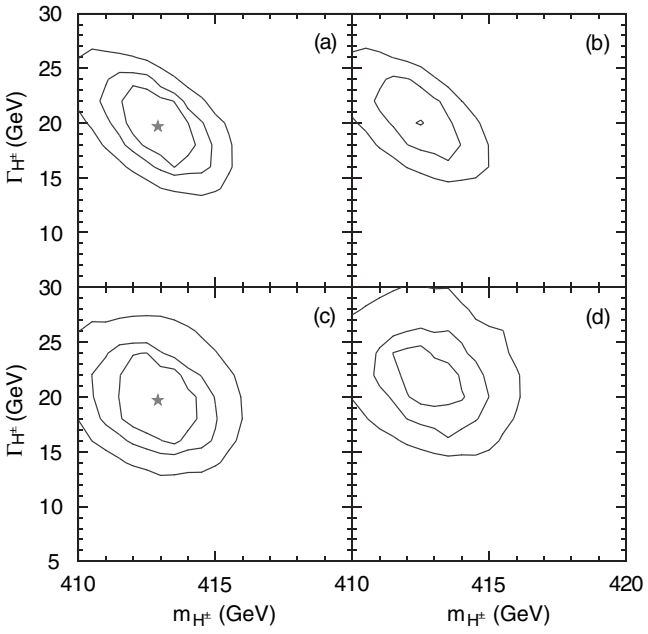

FIG. 8. Contours of constant $\delta\chi^2_{\rm C}$ on $m_{H^\pm}$ vs $\Gamma_{H^\pm}$ planes; $\delta\chi^2_{\rm C} = 1$, 2, and 4 (with $L = 1$ ab^{-1}) from inside. The branching ratio is fixed to be $B_{H^\pm\to bt} = 0.885$ for (a) and (c), and $B_{H^\pm\to bt} = 0.87$ for (b) and (d). Upper two figures ((a) and (b)) are with $tbtb$ mode while the lower ones ((c) and (d)) are without $tbtb$ mode.

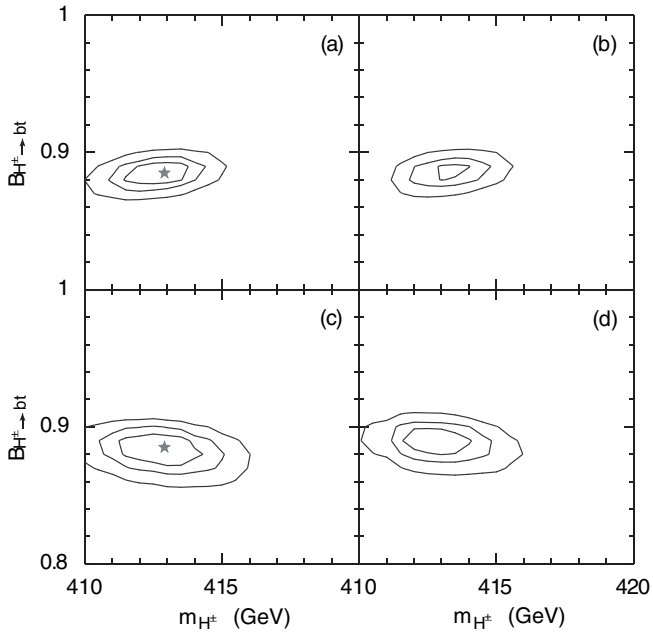

FIG. 9. Contours of constant $\delta\chi^2_{\rm C}$ on $m_{H^\pm}$ vs $B_{H^\pm\to bt}$ planes; $\delta\chi^2_{\rm C} = 1$, 2, and 4 (with $L = 1$ ab^{-1}) from inside. Here, we take $\Gamma_{H^\pm} = 19.7$ GeV for (a) and (c), and $\Gamma_{H^\pm} = 17.0$ GeV for (b) and (d). Upper two figures are with $tbtb$ mode while the lower ones are without $tbtb$ mode.

D. Combined results

Now, we combine the results obtained in the previous subsections. For this purpose, we define the total $\delta\chi^2$ variable as

$$\delta\chi^2_{\rm tot} = \delta\chi^2_{\rm N} + \delta\chi^2_{\rm C}. \tag{3.22}$$

This quantity depends on five parameters (as well as on the underlying parameters); we use m_A, m_H, $m_{H^\pm}$, Γ_A, and $B_{A\to b\bar{b}}$ as free parameters. Once these parameters are fixed, all the Yukawa coupling constants (as well as the QCD correction factors) are determined in the large $\tan\beta$ region and the number of the neutral and charged Higgs production events can be calculated. As we saw in the previous subsections, averaged mass of the neutral Higgses $\bar{m}_{AH}$, the charged Higgs mass $m_{H^\pm}$ and the branching ratios are relatively well determined. Thus, in this subsection, we concentrate on the uncertainties in the remaining two parameters which are most important for the calculation of the relic density of the LSP, i.e., Δm_{AH} and Γ_A.

In Fig. 10, we plot the contours of constant $\delta\chi^2_{\rm tot}$ for point 1 on Δm_{AH} vs Γ_A plane, on which $\bar{m}_{AH}$, $m_{H^\pm}$, and $B_{A\to b\bar{b}}$ are fixed to be the underlying values. As one can see, constraint on the Δm_{AH} vs Γ_A plane becomes more stringent as we add the information from the charged Higgs production events. Compared with Fig. 5, we can see that

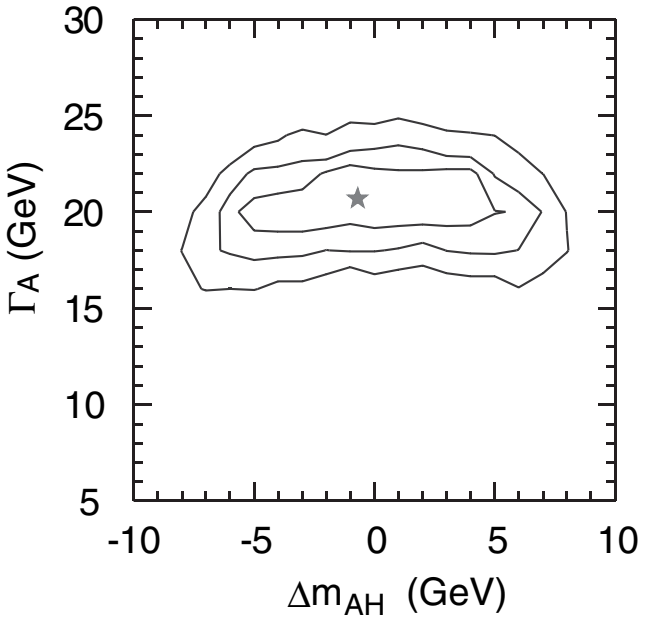

FIG. 10. Contours of constant $\delta\chi^2_{\rm tot}$ for point 1 on Δm_{AH} vs Γ_A plane; $\delta\chi^2_{\rm tot} = 1$, 2, and 4 (with $L = 1$ ab^{-1}) from inside. $\bar{m}_{AH}$, $m_{H^\pm}$, and $B_{A\to b\bar{b}}$ are fixed to be the underlying values.

the errors in Δm_{AH} and Γ_A are reduced by including the information from the charged Higgs productions. We also performed the same study for the point 2, and the result is given in Fig. 11.

Before closing this section, let us comment on the determination of the $\tan\beta$ parameter. Since the decay widths of the heavy Higgses are sensitive to $\tan\beta$, we can obtain information about $\tan\beta$ from the decay widths of the heavy Higgses [9]. In order to derive the value of

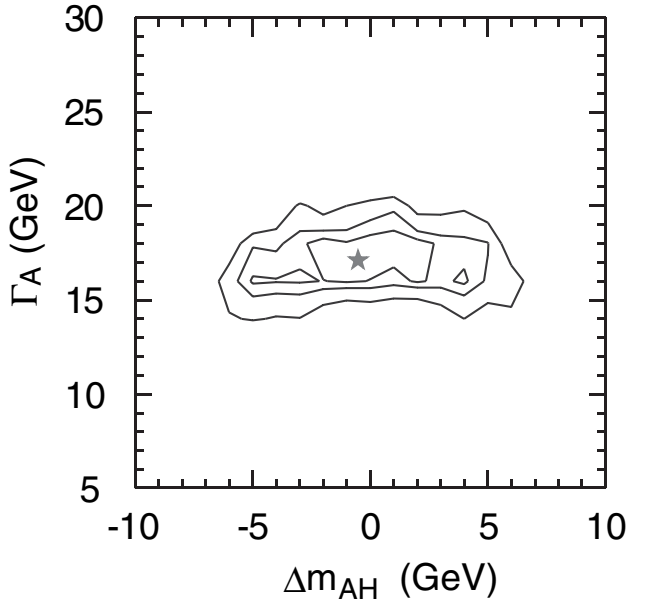

FIG. 11. Same as Fig. 10, but for the point 2.

$\tan\beta$, however, we need to relate the Yukawa coupling constants to the observed masses of the (third-generation) fermions. For the bottom quark, this is difficult since the radiative correction from the supersymmetric diagrams may significantly affect the bottom-quark mass. Expecting that the radiative correction to the mass of τ is small enough, however, we can use the relation

$$\tan\beta = \frac{y_\tau v}{m_\tau}. \tag{3.23}$$

Then, using the decay rate of the CP-odd Higgs boson, for example, we obtain

$$\tan\beta = \sqrt{\frac{16\pi\Gamma_A(1 - B_{A\to b\bar{b}})}{m_A}}\frac{v}{m_\tau}, \tag{3.24}$$

and hence

$$\frac{\delta\tan\beta}{\tan\beta} \simeq \frac{1}{2}\left[\left(\frac{\delta\Gamma_A}{\Gamma_A}\right)^2 + \left(\frac{\delta m_A}{m_A}\right)^2 + \left(\frac{\delta B_{A\to b\bar{b}}}{1 - B_{A\to b\bar{b}}}\right)^2\right]^{1/2}. \tag{3.25}$$

As we have seen in the previous subsections, uncertainties in Γ_A and $B_{A\to\tau\bar{\tau}} = 1 - B_{A\to b\bar{b}}$ are both 10–20% level, while that in m_A is smaller ($\sim 1\%$). Thus, in this case, the $\tan\beta$ parameter can be determined with the accuracy of 10% or so.

IV. RECONSTRUCTION OF DARK-MATTER DENSITY

Now, we are at the position to consider the possibility of reconstructing the dark-matter density in the rapid-annihilation funnels. In the parameter region we are interested in, pair annihilation of the lightest neutralino (which is the LSP) is dominated by the process with the s-channel exchange of the pseudoscalar Higgs boson A. The cross section for this process is calculated as[7]

$$\sigma_{\chi_1^0\chi_1^0\to\text{all}} v_{\rm rel} \simeq \frac{2y^2_{A\chi_1^0\chi_1^0}\Gamma_A}{m_A}\frac{s_{\chi_1^0\chi_1^0}}{(s_{\chi_1^0\chi_1^0} - m_A^2)^2 + \Gamma_A^2 m_A^2}, \tag{4.1}$$

where $s_{\chi_1^0\chi_1^0}$ is the invariant mass of two LSPs in the initial state, and $y_{A\chi_1^0\chi_1^0}$ is the coupling between A and the lightest neutralino, which is given by

$$y_{A\chi_1^0\chi_1^0} = \frac{1}{2}(g_1[U_{\chi^0}]_{11} - g_2[U_{\chi^0}]_{12})(\sin\beta[U_{\chi^0}]_{13} - \cos\beta[U_{\chi^0}]_{14}). \tag{4.2}$$

Here, U_{χ^0} is the unitary matrix which diagonalizes the neutralino mass matrix which is given by

[7]Strictly speaking, in Eq. (4.1), we have to take account of the QCD correction to the decay rate Γ_A when $s^{1/2}_{\chi_1^0\chi_1^0}$ differs from m_A. Such a QCD correction is calculable and, in this paper, we neglect such a correction.

$$\mathcal{M}_0 = \begin{pmatrix} -m_{\rm G1} & 0 & -g_1 v\cos\beta & g_1 v\sin\beta \\ 0 & -m_{\rm G2} & g_2 v\cos\beta & -g_2 v\sin\beta \\ -g_1 v\cos\beta & g_2 v\cos\beta & 0 & \mu_H \\ g_1 v\sin\beta & -g_2 v\sin\beta & \mu_H & 0 \end{pmatrix}, \tag{4.3}$$

with $m_{\rm G1}$, $m_{\rm G2}$, and μ_H being the gaugino masses for $U(1)_Y$ and $SU(2)_L$ gauge groups and SUSY invariant Higgs mass, respectively. Thus, in the rapid-annihilation funnels, dominant contribution to the pair annihilation cross section of the lightest neutralino is calculated once m_A and Γ_A as well as $y_{A\chi_1^0\chi_1^0}$ are determined. In the previous section, we have seen that, by the study of the heavy Higgses, m_A and Γ_A are constrained fairly well.

For the determination of $y_{A\chi_1^0\chi_1^0}$, we need the mixing matrix U_{χ^0} (as well as $\tan\beta$) which is calculated from the neutralino mass matrix. Importantly, the neutralino mass matrix depends on the gaugino masses and the SUSY invariant Higgs mass which can be determined once the chargino and neutralino masses are experimentally measured. At the ILC, measurements of these masses can be performed if the charginos and neutralinos are kinematically accessible. In particular, by studying the production processes at the threshold region (i.e., by the threshold scan), some of the masses of the charginos and neutralinos can be determined with the accuracy of ~50 MeV [3]. In addition, from the kinematics of the decay products of the chargino and neutralinos (as well as sfermions, if kinematically accessible), mass of the LSP (i.e., the lightest neutralino) is also determined with $\delta m_{\chi_1^0} \sim 50$ MeV [3]. Thus, if all the charginos and neutralinos are seen at the ILC, it will give us enough information to precisely determine $y_{A\chi_1^0\chi_1^0}$. If some of the charginos or the neutralinos are too heavy to be experimentally produced, it becomes rather difficult to determine the neutralino mixing parameters. In such a case, we may have to perform some global fit using all the masses of the superparticles. Of course, some information from the LHC may be also used. Since our main concern is to study the properties of the heavy Higgses, we do not consider the detail of the parameters in the neutralino sector. Instead, we assume that, at the ILC, all the charginos and neutralinos can be produced and that their masses can be precisely measured. If the masses of all the charginos and neutralinos are measured with the accuracy of ~50 MeV, the uncertainty of $y_{A\chi_1^0\chi_1^0}$ is expected to be O(0.01%) so that the dominant uncertainty in the reconstructed value of $\Omega_{\rm LSP}$ is from m_A and Γ_A.

To see how well we can reconstruct $\Omega_{\rm LSP}$, in Figs. 12 and 13, we plot theoretically calculated value of $\Omega_{\rm LSP}$ on m_A vs Γ_A plane. (In our numerical calculation, we use the DARKSUSY package [43] to calculate $\Omega_{\rm LSP}$.) Here, we fixed $y_{A\chi_1^0\chi_1^0}$ and $m_{\chi_1^0}$ as their underlying values and calculated $\Omega_{\rm LSP}$ as a function of m_A and Γ_A. In the same figure, we also show the constraint on the m_A vs Γ_A plane expected from the ILC. Here, assuming that the dominant error of m_A is from Δm_{AH}, we neglected the uncertainty of $\bar{m}_{AH}$. From these figures, we can see that the uncertainty of $\Omega_{\rm LSP}$ is 10–20%, which is comparable to the uncertainty of the dark-matter density determined from the WMAP data.

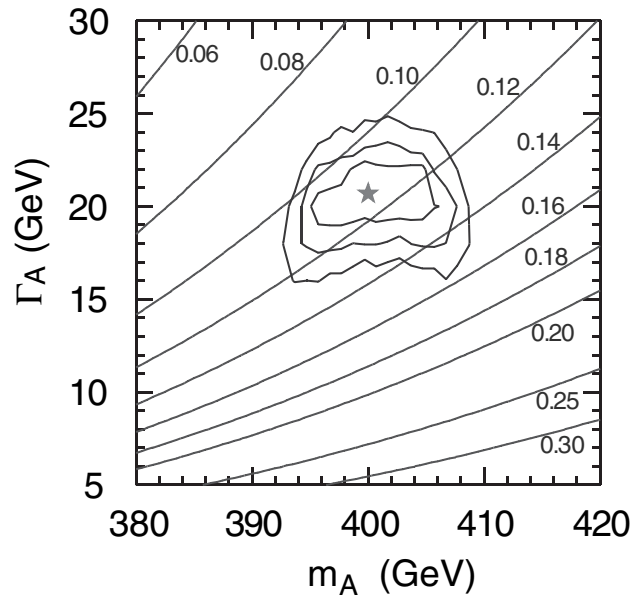

FIG. 12. Contours of constant thermal relic density of the LSP on the m_A vs Γ_A plane for the point 1. The numbers in the figure are the value of $\Omega_{\rm LSP}h^2$. Contours surrounding the star indicate the expected constraints on the m_A vs Γ_A plane from the ILC ($\delta\chi^2_{\rm tot} = 1$, 2, and 4 from inside, with $L = 1$ ab^{-1}).

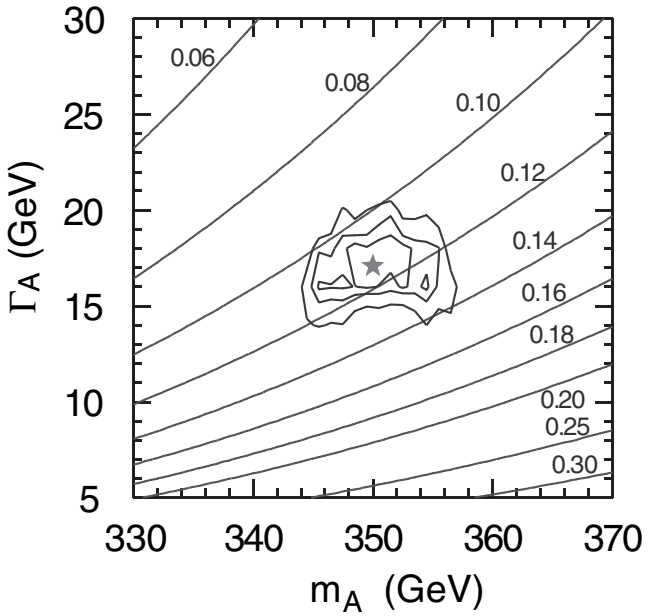

FIG. 13. Same as Fig. 12 but for point 2.

We have not discussed possible errors of $\Omega_{\rm LSP}$ originating from parameters other than m_A, Γ_A, and $y_{A\chi_1^0\chi_1^0}$. In order to calculate the total pair annihilation cross section of the LSP, we also have to take account of other processes like the s-channel H^0 exchange and t-channel sfermion exchange processes. In the rapid-annihilation funnels, however, effects of these processes are subdominant. (We have checked that processes other than the CP-odd Higgs exchange change the value of $\Omega_{\rm LSP}$ at most a few % in points 1 and 2.) In addition, more importantly, once the properties of the heavy Higgses and the sfermions are determined at the ILC, cross sections for these subdominant processes are also calculated. Thus, we expect that the uncertainty in $\Omega_{\rm LSP}$ from the processes other than the CP-odd Higgs exchange is less than a few % and that the dominant errors are from m_A and Γ_A.

V. CONCLUSIONS AND DISCUSSION

We have considered the capability of the e^+e^- linear collider for studying the properties of the heavy Higgs bosons in the supersymmetric standard model at the ILC. We concentrated on the large $\tan\beta$ region which is motivated, in particular, by explaining the dark-matter density of the universe (i.e., so-called ''rapid-annihilation funnels''). We perform a systematic analysis to estimate expected uncertainties in the determination of the masses and widths of the heavy Higgs bosons.

With the study of the invariant-mass distributions of the jets in the final state, we have seen that the masses, widths, and the branching ratios of the heavy Higgses are well constrained. Compared to the averaged value $\bar{m}_{AH} = \frac{1}{2} \times (m_A + m_H)$, mass difference of the neutral Higgses, $\Delta m_{AH} = \frac{1}{2}(m_A - m_H)$, is more difficult to measure. Consequently, if we try to experimentally determine the masses of the neutral heavy Higgses, uncertainty in Δm_{AH} becomes the significant source of the error.

In this paper, our primary purpose was to point out the strategy for the systematic study of the heavy Higgs bosons at the ILC and to estimate the expected uncertainties in the measurements of their masses and widths. Thus, we assumed that the b-tagging efficiency and the energy resolution of the detector is well understood and we did not consider systematic errors from these. In addition, for the background, we take account only of the dominant physics background. When the study suggested in this paper will be performed, these points should be studied in more detail; in order to realize the detailed and precise study of the heavy Higgs bosons, the following will be necessary:

(a) Good understanding and high efficiency of the b-tagging.
(b) High resolution of, in particular, hadron calorimeter.
(c) Good understanding of the backgrounds.

We have also discussed the implication of the study of the heavy Higgses to the calculation of the relic density of the LSP. In the rapid-annihilation funnels, the dominant pair annihilation process of the LSP is through the s-channel exchange of the CP-odd Higgs boson. In this case, the mass and width of the CP-odd Higgs boson should be determined for the precise calculation of the relic density of the LSP. We have seen that, if the LSP dark matter is realized in the rapid-annihilation funnels, the the dark-matter density can be reconstructed with a very good accuracy of $10 - 20\%$ (see Figs. 12 and 13). If the uncertainty in the mass or the width of the CP-odd Higgs can be reduced, we will have a better determination of $\Omega_{\rm LSP}$. In particular, the dominant source of the uncertainty in m_A is from the determination of the mass difference of two neutral heavy Higgses. If the radiative correction to the Higgs potential is well understood, then the mass difference Δm_{AH} may be theoretically calculated. In this case, uncertainty in m_A becomes smaller and a better determination of $\Omega_{\rm LSP}$ is expected. In addition, we have also assumed that the radiative corrections to the pair annihilation processes of the LSP will become well studied by the time when the superparticles as well as the heavy Higgses are produced at the ILC. Although most of the radiative corrections are calculable, many of them have not been calculated yet. In order for the precise theoretical calculation of $\Omega_{\rm LSP}$, such a study will be very important.

In conclusion, we have seen that the ILC is very useful not only for studying the properties of the new particles in particle-physics models beyond the standard model (in this case, the heavy Higgse in the sypersymmetric models) but also to have deeper insights into the evolution of the universe. In particular, the ILC may help answering one of the most serious mysteries in cosmology, the origin of the dark matter of the universe. If the reconstruction of the dark-matter density will be successful, it will provide us a better understanding of our universe up to the temperature of O(10 GeV).

ACKNOWLEDGMENTS

This work is supported in part by the 21st century COE program, ''Exploring New Science by Bridging Particle-Matter Hierarchy.'' The work of T. M. is also supported by the Grants-in-Aid of the Ministry of Education, Science, Sports, and Culture of Japan No. 15540247.

[1] S. Matsumoto *et al.* (JLC Group), ''JLC-1,'' KEK Report 92–16, 1992.
[2] S. Kuhlman *et al.* (NLC ZDR Design Group and NLC Physics Working Group), ''Physics and Technology of the Next Linear Collider,'' BNL 52-502 (1996).
[3] J. A. Aguilar-Saavedra *et al.* (ECFA/DESY LC Physics Working Group), hep-ph/0106315.
[4] For the recent activities, see also the web page of *Proceedings of the International Linear Collider Physics and Deterctor Workshop and Second ILC Accelerator Workshop, Snowmass, Colorado, 2005*, http://alcpg2005.colorado.edu.
[5] A. Djouadi, J. Kalinowski, P. Ohmann, and P. M. Zerwas, Z. Phys. C **74**, 93 (1997).
[6] J. F. Gunion and J. Kelly, Phys. Rev. D **56**, 1730 (1997).
[7] J. L. Feng and T. Moroi, Phys. Rev. D **56**, 5962 (1997).
[8] V. D. Barger, T. Han, and J. Jiang, Phys. Rev. D **63**, 075002 (2001).
[9] J. F. Gunion, T. Han, J. Jiang, and A. Sopczak, Phys. Lett. B **565**, 42 (2003).
[10] K. Desch, T. Klimkovich, T. Kuhl, and A. Raspereza, hep-ph/0406229.
[11] H. Baer *et al.*, J. High Energy Phys. 07 (2002) 050.
[12] J. R. Ellis, K. A. Olive, Y. Santoso, and V. C. Spanos, Phys. Lett. B **565**, 176 (2003).
[13] H. Baer and C. Balazs, J. Cosmol. Astropart. Phys. 05 (2003) 006.
[14] U. Chattopadhyay, A. Corsetti, and P. Nath, Phys. Rev. D **68**, 035005 (2003).
[15] A. B. Lahanas and D. V. Nanopoulos, Phys. Lett. B **568**, 55 (2003).
[16] H. Baer *et al.*, J. High Energy Phys. 06 (2003) 054.
[17] M. Battaglia *et al.*, Eur. Phys. J. C **33**, 273 (2004).
[18] G. Belanger *et al.*, Nucl. Phys. **B706**, 411 (2005).
[19] E. A. Baltz and P. Gondolo, J. High Energy Phys. 10 (2004) 052.
[20] C. L. Bennett *et al.*, Astrophys. J. Suppl. Ser. **148**, 1 (2003).
[21] S. Eidelman *et al.* (Particle Data Group), Phys. Lett. B **592**, 1 (2004).
[22] M. Battaglia, hep-ph/0410123.
[23] B. C. Allanach, G. Belanger, F. Boudjema, and A. Pukhov, J. High Energy Phys. 12 (2004) 020.
[24] P. Bambade, M. Berggren, F. Richard, and Z. Zhang, hep-ph/0406010.
[25] V. Khotilovich, R. Arnowitt, B. Dutta, and T. Kamon, Phys. Lett. B **618**, 182 (2005).
[26] T. Moroi, Y. Shimizu, and A. Yotsuyanagi, Phys. Lett. B **625**, 79 (2005).
[27] M. Carena *et al.*, hep-ph/0508152 [Phys. Rev. D (to be published)].
[28] A. Birkedal *et al.*, hep-ph/0507214.
[29] M. Battaglia and M. E. Peskin, hep-ph/0509135.
[30] M. Drees *et al.*, Phys. Rev. D **63**, 035008 (2001).
[31] M. Battaglia, I. Hinchliffe, and D. Tovey, J. Phys. G **30**, R217 (2004).
[32] G. Polesello and D. R. Tovey, J. High Energy Phys. 05 (2004) 071.
[33] P. Janot (CMS Collaboration), hep-ph/0406275.
[34] H. Baer, A. Belyaev, T. Krupovnickas, and J. O'Farrill, J. Cosmol. Astropart. Phys. 08 (2004) 005.
[35] See, for example, J. F. Gunion, H. E. Haber, G. L. Kane, and S. Dawson, Report No. SCIPP-89/13.
[36] L. J. Hall, R. Rattazzi, and U. Sarid, Phys. Rev. D **50**, 7048 (1994).
[37] M. Carena, M. Olechowski, S. Pokorski, and C. E. M. Wagner, Nucl. Phys. **B426**, 269 (1994).
[38] E. Braaten and J. P. Leveille, Phys. Rev. D **22**, 715 (1980).
[39] M. Drees and K. I. Hikasa, Phys. Lett. B **240**, 455 (1990); **262**, 497E (1991).
[40] F. E. Paige, S. D. Protopescu, H. Baer, and X. Tata, hep-ph/0312045.
[41] S. Yamashita, *Proceedings of the International Linear Collider Physics and Deterctor Workshop and Second ILC Accelerator Workshop, Snowmass, Colorado, 2005* http://alcpg2005.colorado.edu.
[42] E. Boos *et al.* (CompHEP Collaboration), Nucl. Instrum. Methods Phys. Res., Sect. A **534**, 250 (2004).
[43] P. Gondolo *et al.*, J. Cosmol. Astropart. Phys. 07 (2004) 008.